Electron spin resonance in Eu-based iron pnictides

H.-A. Krug von Nidda,[1] S. Kraus,[1] S. Schaile,[1] E. Dengler,[1] N. Pascher,[1] M. Hemmida,[1] M. J. Eom,[2] J. S. Kim,[2] H. S. Jeevan,[3] P. Gegenwart,[3] J. Deisenhofer,[1] and A. Loidl[1]

[1]*Experimentalphysik V, Center for Electronic Correlations and Magnetism, Institute for Physics, Augsburg University, D-86135 Augsburg, Germany*

[2]*Department of Physics, Pohang University of Science and Technology, Pohang 790-784, Korea*

[3]*I. Physik. Institut, Georg-August-Universität Göttingen, D-37077 Göttingen, Germany*

(Received 11 May 2012; revised manuscript received 3 August 2012; published 10 September 2012)

The phase diagrams of $EuFe_{2-x}Co_xAs_2$ ($0 \leqslant x \leqslant 0.4$) and $EuFe_2As_{2-y}P_y$ ($0 \leqslant y \leqslant 0.43$) are investigated by Eu^{2+} electron spin resonance (ESR) in single crystals. From the temperature dependence of the linewidth $\Delta H(T)$ of the exchange narrowed ESR line, the spin-density wave (SDW) ($T < T_{SDW}$) and the normal metallic regime ($T > T_{SDW}$) are clearly distinguished. At $T > T_{SDW}$ the isotropic linear increase of the linewidth is driven by the Korringa relaxation which measures the conduction-electron density of states at the Fermi level. For $T < T_{SDW}$ the anisotropy probes the local ligand field, while the coupling to the conduction electrons is strongly weakened. With increasing substitution of x or y the transition temperature T_{SDW} decreases linearly accompanied by a linear decrease of the Korringa-relaxation rate from 8 Oe/K at $x = y = 0$ down to 3 Oe/K at the onset of superconductivity. For $x > 0.2$ and $y > 0.3$ it remains nearly constant. Comparative ESR measurements on single crystals of the Eu diluted SDW compound $Eu_{0.2}Sr_{0.8}Fe_2As_2$ and superconducting (SC) $Eu_{0.22}Sr_{0.78}Fe_{1.72}Co_{0.28}As_2$ corroborate the leading influence of the ligand field on the Eu^{2+} spin relaxation in the SDW regime as well as the Korringa relaxation in the normal metallic regime. A coherence peak is not detected in the latter compound below $T_c = 21$ K, which is in agreement with the expected complex anisotropic SC gap structure. In contrast, indications for phase coexistence and BCS-type superconductivity are found in $EuFe_2As_{1.57}P_{0.43}$.

DOI: 10.1103/PhysRevB.86.094411 PACS number(s): 74.70.Xa, 75.30.Fv, 76.30.−v

I. INTRODUCTION

Iron-based pnictides and chalcogenides became a central topic of modern solid-state physics when in 2008 superconductivity was discovered in $LaFeAsO_{1-x}F_x$ with transition temperatures as high as $T_c = 26$ K,[1] as well as in $SmFeAsO_{1-x}F_x$ ($T_c = 55$ K),[2,3] in $Ba_{1-x}K_xFe_2As_2$ ($T_c = 38$ K),[4,5] and in α-$FeSe_{1-x}$ ($T_c = 8$ K).[6] Apparently the superconductivity emerges from the FeAs or FeSe layers which are the building blocks of the corresponding quasi-two-dimensional crystal structures suggesting the analogy to the cuprate-based high-T_c superconductors. Similar to the cuprates, the mother compounds ($x = 0$) exhibit an antiferromagnetic ground state—here usually a spin-density wave (SDW)—which under doping ($x > 0$) becomes gradually suppressed and gives rise to a superconducting dome. However, in the iron-based superconductors the parent phases usually are metallic. Early reviews on the enormous research activities to understand the origin of the superconductivity and its interplay with the magnetism of iron in these compounds are given by Johnston[7] and Stewart.[8]

The ternary AFe_2As_2 (122) systems (with A = Ba, Sr, Ca, Eu), which crystallize in the tetragonal $ThCr_2Si_2$ structure, can be driven from the SDW ground state into superconductivity by chemical substitution on each of the lattice sites, e.g., substituting the A-site ions by K,[4,9] or Fe by Co,[10,11] as well as As by P.[12,13] Special attention is devoted to $EuFe_2As_2$ showing the highest reported SDW transition temperature $T_{SDW} = 190$ K in the pnictides, while antiferromagnetic order of the europium spins is observed only below $T_N = 19$ K.[14–16]

The antiferromagnetic structure of $EuFe_2As_2$ was investigated by means of magnetic resonant x-ray scattering and neutron scattering.[17–19] The SDW transition, which is accompanied by an orthorhombic structural distortion, was found to be weakly of first order, while the ordering of the Eu moments was characterized as second-order phase transition. Ferromagnetic Eu^{2+} layers are coupled antiferromagnetically along the c axis with the europium moments aligned along the a axis. The iron moments are aligned along the a axis as well, but directed antiparallel on neighboring sites along a and c. Optical spectroscopy probed the opening of the SDW gap,[16] which even turned out to consist of two gaps related to different electronic subsystems.[20] The complex electronic structure is further elucidated by angular-resolved photoelectron spectroscopy (ARPES) which reveals dropletlike Fermi surfaces in the SDW state of the iron system.[21] Nevertheless, there have been no detectable changes across the antiferromagnetic ordering of the Eu spins, indicating only a weak coupling between both systems.[22] External magnetic fields reorient the Eu spins into a ferromagnetic phase already below 2 T,[23] but do not affect the iron moments at least up to highest applied fields of 55 T.[24] Magnetotransport measurements show that electron scattering due to the Eu^{2+} local moments plays only a minor role for the electronic transport properties of $EuFe_2As_2$.[25] Both observations again are in accordance with weak coupling between Fe spins and Eu spins.

Application of hydrostatic pressure to $EuFe_2As_2$ (Refs. 26–32) as well as isovalent P substitution in $EuFe_2As_{2-y}P_y$ (Refs. 13 and 33–38) suppress the SDW state, give rise to superconductivity for $24 < p < 31$ kbar[30] and $0.32 < y < 0.44$,[13] and yield ferromagnetic Eu order at higher pressure and P concentration, respectively. The electron doping by substitution of Fe by Co revealed a comparable behavior,[39–43] but the superconducting transition remains incomplete in the resistivity. Moreover, suppression of the SDW transition and emergence of ferromagnetic ordering of the Eu^{2+}

moments was found in $EuFe_{2-x}Ni_xAs_2$, but without any superconducting phase.[45] On the other hand, dilution of the Eu system is in favor of superconductivity as observed, e.g., in $Eu_{0.5}K_{0.5}Fe_2As_2$ with $T_c = 32$ K,[9] in $Eu_{0.7}Na_{0.3}Fe_2As_2$ with $T_c = 34.7$ K,[46] and under hydrostatic pressure in $Eu_{0.5}Ca_{0.5}Fe_2As_2$ with $T_c \approx 20$ K above 12.7 kbar.[47]

Electron spin resonance (ESR) at the Eu^{2+} spins turned out to be very sensitive to the local electronic density of states. In single crystalline $EuFe_2As_2$ previous ESR investigations revealed a drastic change in the spin relaxation of the europium system at T_{SDW}: The Korringa-type linear increase of the linewidth with temperature typical for metals above T_{SDW} is strongly suppressed below T_{SDW} indicating the opening of a gap in the conduction electron density of states at the Eu site.[48] First ESR investigations of the Co substitutional series at temperatures above 77 K indicate a linear relation between the Korringa slope at high temperatures and both the SDW transition temperature T_{SDW} and the superconducting transition temperature T_c.[49] In $Eu_{0.5}K_{0.5}Fe_2As_2$, where the SDW is completely suppressed by hole doping and superconductivity is found below $T_c = 32$ K,[9] the ESR signal of the Eu^{2+} spins gives direct access to the superconducting state: Below T_c the spin-lattice relaxation rate followed a superlinear law $1/T_1^{ESR} \propto T^{1.5}$. At the same time no Hebel-Slichter peak was observed, ruling out a simple isotropic BCS scenario in this compound.[50]

In the present work, we report a comprehensive study of the influence of cobalt and phosphorus substitution as well as dilution of europium on the ESR properties of $EuFe_2As_2$ single crystals in the temperature range $4.2 \leqslant T \leqslant 300$ K. The aim is to study systematically the evolution of the dynamic susceptibility of the itinerant Fe spins from SDW formation to superconductivity. The g value of the Eu^{2+}-ESR signal probes the homogeneous polarization of the Fe spins in the external field, and thus its shift from the free ionic g value yields the local static susceptibility of the itinerant electrons.[51,52] The linewidth of the Eu signal measures the imaginary part of the dynamic susceptibility of the Fe spins as follows from the fluctuation-dissipation theorem.[52–55] These quantities will give information on the band structure close to the Fermi energy and the gap formation at the transition into the SDW as well as SC phases, which are topics currently under debate to understand the character of superconductivity in iron pnictides.

II. EXPERIMENTAL DETAILS

Single crystals of $EuFe_{2-x}Co_xAs_2$ $(0 \leqslant x \leqslant 0.4)$ and $EuFe_2As_{2-y}P_y$ $(0 \leqslant y \leqslant 0.43)$—as well as two single crystals ($x = 0$ and 0.28) with about 80% Sr on the Eu site—were prepared by flux technique and Bridgeman method as described in Refs. 48 and 13, respectively. Most of the ESR measurements were performed in a Bruker ELEXSYS E500 CW spectrometer at X-band frequencies ($\nu \approx 9.36$ GHz) in the temperature region $4.2 < T < 300$ K using an Oxford Instruments ESR 900 continuous He gas-flow cryostat. ESR detects the power P absorbed by the sample from the transverse magnetic microwave field as a function of the static magnetic field H. The signal-to-noise ratio of the spectra is improved by recording the derivative dP/dH using lock-in technique with field modulation. The single crystals were fixed in Suprasil (Heraeus) quartz tubes by paraffin with the c axis parallel or perpendicular to the axis of the quartz tube. A Bruker programmable goniometer driven by a step motor allowed for orientation-dependent measurements with a precision better than 1°. For $x = 0.3$ comparative ESR experiments have been performed at Q-band frequency ($\nu \approx 34.1$ GHz) in Augsburg as well as at L-band frequency ($\nu \approx 1.09$ GHz) at the Bruker ELEXSYS spectrometer in Dresden.

III. EXPERIMENTAL RESULTS AND DISCUSSION

A. Co substitution on the Fe site

Due to its half-filled $4f$ shell, Eu^{2+} exhibits a pure S state with spin $S = 7/2$. Because of the zero orbital momentum the direct relaxation to the lattice practically vanishes, and therefore, the paramagnetic resonance line can be well resolved up to room temperature. Figure 1 shows ESR spectra of three $EuFe_{2-x}Co_xAs_2$ single crystals with different Co concentrations x in the paramagnetic regime at a temperature of $T = 50$ K for the magnetic field H applied both parallel and perpendicular to the crystallographic c axis. As in the mother compound[48] (see also upper frames of Fig. 8) all spectra consist of a single exchange-narrowed resonance line—i.e., any line splitting or inhomogeneous broadening is averaged out by the isotropic exchange interaction—which narrows on increasing Co concentration x. The resonance line is well described by a Dyson shape,[56] which corresponds to a Lorentz line at resonance field H_{res} with half width at half maximum ΔH and a contribution of dispersion to the absorption given by the (D/A) ratio $0 \leqslant D/A \leqslant 1$. The dispersion results in an

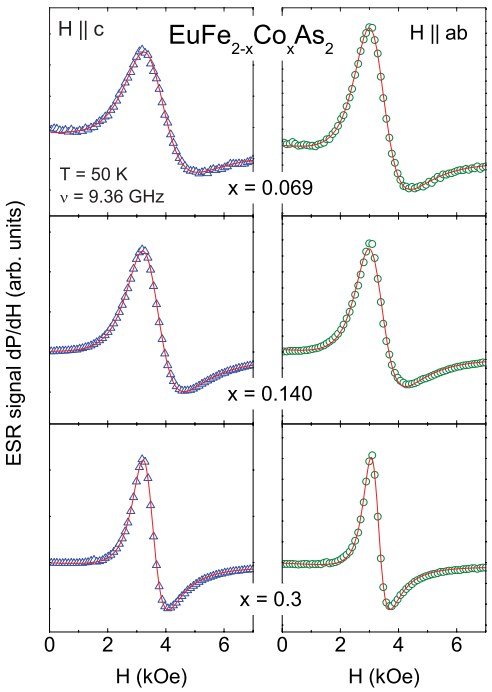

FIG. 1. (Color online) ESR spectra obtained on single crystals of $EuFe_{2-x}Co_xAs_2$ with $x = 0.069$ (upper), 0.140 (middle), and 0.3 (lower frames) at $T = 50$ K for the magnetic field applied parallel (left column) or perpendicular (right column) to the tetragonal c axis. Red solid lines indicate the fit by a Dyson shape.

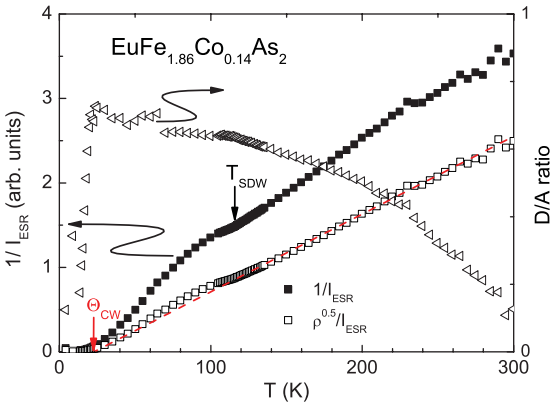

FIG. 2. (Color online) Dispersion-to-absorption ratio (right ordinate) and inverse ESR intensity (left ordinate) before (closed squares) and after (open squares) skin-depth correction for a single crystal $EuFe_{1.86}Co_{0.14}As_2$. The red dashed line indicates a Curie-Weiss-like behavior.

asymmetry typical for metals, where due to the conductivity the skin effect drives electric and magnetic components of the microwave field out of phase in the sample. The D/A ratio depends on the sample size, geometry, and skin depth. If the skin depth is small compared to the sample size, D/A approaches 1; in the reverse case D/A vanishes as in insulators. As the linewidth ΔH is of the same order of magnitude as the resonance field $H_{\rm res}$, the counter resonance at $-H_{\rm res}$ was included in the fitting process as well.[57]

Figure 2 exemplarily illustrates the typical temperature dependence for D/A ratio and inverse ESR intensity as obtained for the cobalt concentration $x = 0.14$. Similar to pure $EuFe_2As_2$ (Ref. 48) the D/A ratio increases on decreasing temperature from about 0.1 at room temperature up to 0.7 below 100 K due to the decreasing electrical resistivity. A significant drop marks the onset of magnetic order, which is accompanied by a change in signal shape due to strong demagnetization effects. These are strongly dependent on details of sample shape and surface, and therefore will not be considered further. The inverse intensity $1/I_{\rm ESR}$ monotonously increases with increasing temperature and—after correction by the skin depth $\propto\sqrt{\rho/\nu}$ with the resistivity (ρ) data[49] and microwave frequency $\nu = 9.36$ GHz—nicely resembles the expected Curie-Weiss law $1/I_{\rm ESR} \propto (T - \Theta_{\rm CW})$ with $\Theta_{\rm CW} \approx 22$ K, except for a slight shift below the SDW transition at $T_{\rm SDW} \approx 120$ K.

The most important information is obtained from the temperature dependence of the linewidth and the resonance field depicted in Figs. 3 and 4 for the magnetic field aligned along the three principal crystal axes. For completeness we added the data of pure $EuFe_2As_2$. Up to $x = 0.171$ one clearly recognizes the SDW transition at $T_{\rm SDW}$, which separates the usual metallic Korringa-relaxation regime at high temperatures from the insulatorlike relaxation regime at low temperatures. Moreover, the resonance field significantly shifts on approaching magnetic order of the Eu spins at $T_{\rm N}$ due to the increasing demagnetization fields. At the same time the linewidth strongly increases because of critical magnetic fluctuations close to the phase transition.

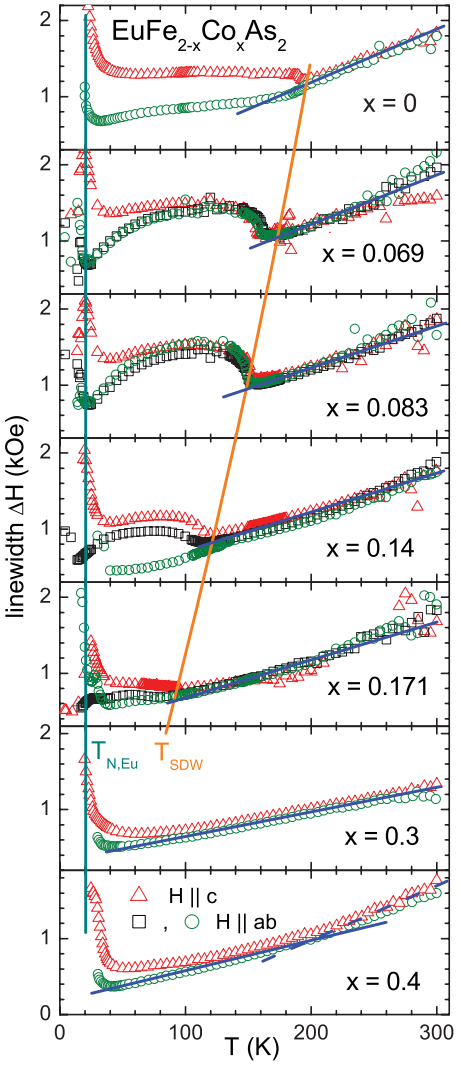

FIG. 3. (Color online) Temperature dependence of the ESR linewidth ΔH in $EuFe_{2-x}Co_xAs_2$ for $0 \leqslant x \leqslant 0.4$ for the magnetic field aligned along the principal axes. The concentration dependence of the SDW transition ($T_{\rm SDW}$) and of the magnetic ordering transition of the Eu spins ($T_{\rm N,Eu}$) is illustrated by solid lines. The straight solid lines in each graph indicate the linear Korringa law.

In contrast to the isotropy of the parameters above the SDW transition, below $T_{\rm SDW}$ both linewidth and resonance field develop a pronounced spatial anisotropy. In the SDW state only the dipolar interaction between the Eu spins and the crystal-electric field of the ligands determine the spin relaxation like in an insulator. While for $x = 0$ the anisotropy shows up directly on crossing $T_{\rm SDW}$ down to lower temperatures, one only observes a strong increase of the linewidth for $x = 0.069$ and $x = 0.083$ followed by a rather temperature-independent regime. Only at lower temperatures ($T < T_{\rm SDW}/2$) does the tetragonal symmetry show up. This is probably a consequence of the disorder induced by the Co substitution, which randomly disturbs the local crystal field and its symmetry axis leading to an averaged broadening. Note, however, that for $x \leqslant 0.1$ the absolute value of the linewidth in this intermediate regime approximates the value of the plateau for $H \parallel c$ at $x = 0$, indicating a comparable magnitude of the uniaxial zero-field

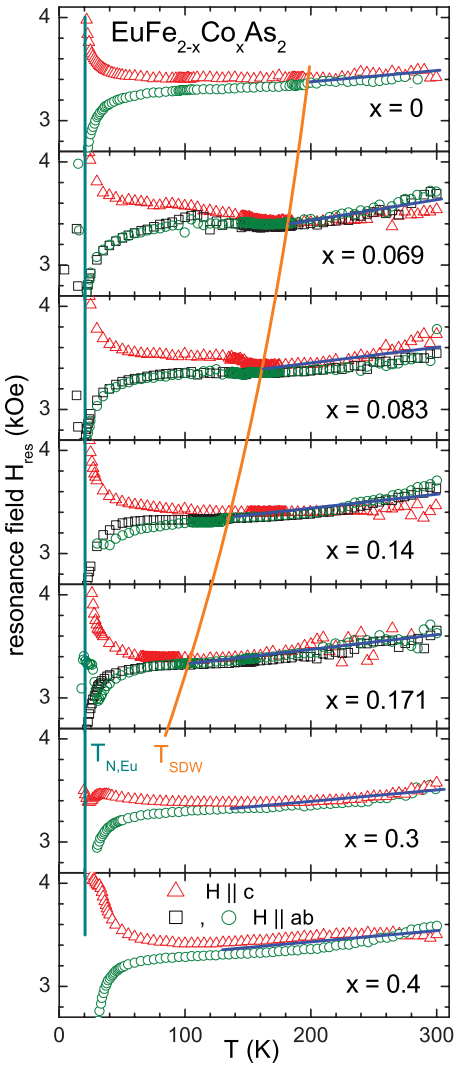

FIG. 4. (Color online) Temperature dependence of the resonance field $H_{\rm res}$ in $EuFe_{2-x}Co_xAs_2$ for $0 \leqslant x \leqslant 0.4$ for the magnetic field aligned along the principal axes. The concentration dependence of the SDW transition ($T_{\rm SDW}$) and of the magnetic ordering transition of the Eu spins ($T_{\rm N,Eu}$) is illustrated by solid lines. The blue solid lines in each graph are guides for the eye.

splitting parameter D, which was determined as $D \approx 5.5$ GHz in $EuFe_2As_2$.[48]

Taking a closer look to the anisotropy in the SDW phase one recognizes the evolution of an orthorhombic contribution in contrast to the purely tetragonal symmetry in $EuFe_2As_2$.[48] This develops on increasing Co concentration x as illustrated in Fig. 5. While for $x = 0.069$ the symmetry is still tetragonal, a strong orthorhombic component shows up for $x = 0.170$. Note that this development is best visible in the linewidth data, while the symmetry of the resonance field is basically determined by demagnetization: for the platelet-shaped samples under investigation the resonance shifts to higher fields in the case of a magnetic field applied perpendicular to the plane, but to lower fields, if it is applied within the plane.[58] Indeed, the anisotropy of the linewidth is expected to exhibit an orthorhombic symmetry in the whole SDW regime due to the structural transition which accompanies the formation of

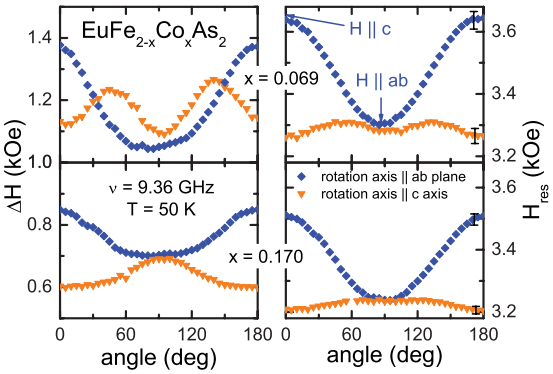

FIG. 5. (Color online) Angular dependence of linewidth (left frames) and resonance field (right frames) for $EuFe_{2-x}Co_xAs_2$ single crystals with $x = 0.069$ and 0.170 at $T = 50$ K.

the SDW. However, the single crystals are usually heavily twinned in the *ab* plane, as has been revealed by Tanatar *et al.*[59] using polarized light microscopy and spatially resolved high-energy synchrotron x-ray diffraction. Nevertheless, the in-plane anisotropy of the resistivity was investigated by Chu *et al.*[60] in single crystals of $BaFe_{2-x}Co_xAs_2$ which were detwinned by means of uniaxial stress. In the SDW phase a significant anisotropy shows up with the resistivity along the shorter b axis being larger than along the a axis. The in-plane anisotropy is only weak in the pure system ($x = 0$) but reaches a maximum value of about 2 for compositions close to the onset of the superconducting dome. Our ESR data which probe the anisotropy on a local atomic scale are in accordance with this finding regarding the data of the at least partially untwinned crystals with $x = 0.140$ and $x = 0.171$.

As already observed in pure $EuFe_2As_2$ the linewidth and resonance field are practically independent of the orientation of the magnetic field above $T_{\rm SDW}$. Here the linewidth increases approximately linearly with temperature indicating the Korringa relaxation of the localized Eu^{2+} spins via scattering of the conduction electrons[56]

$$\Delta H = bT = \frac{\pi k_{\rm B}}{g\mu_{\rm B}} \langle J^2(q) \rangle N^2(E_{\rm F}) T, \qquad (1)$$

where $\langle J^2(q) \rangle$ denotes the squared exchange constant between localized spins and conduction electrons averaged over the momentum transfer q, $N(E_{\rm F})$ is the conduction-electron density of states at the Fermi energy $E_{\rm F}$, $\mu_{\rm B}$ denotes the Bohr magneton, and $k_{\rm B}$ the Boltzmann constant. With increasing Co concentration x the Korringa slope b, which is depicted in Fig. 6, decreases from $b \approx 8$ Oe/K until the SDW is suppressed and remains approximately constant at about $b \approx 3$ Oe/K for higher x values in good agreement with the results of Ying *et al.*,[49] who pointed out the empirical relation between b and $T_{\rm SDW}$. Looking closer to the increase of the linewidth, it turns out to be slightly stronger than linear with temperature. This effect is most pronounced for $x = 0.4$, where the slope of the linewidth above 200 K is higher by a factor of about 2 as compared to temperatures below 200 K. An analogous result was obtained from ^{75}As nuclear magnetic resonance (NMR) measurements in $BaFe_{2-x}Co_xAs_2$, where in the normal metallic phase the nuclear spin-lattice relaxation rate $1/T_1$ was found to deviate from the linear temperature law

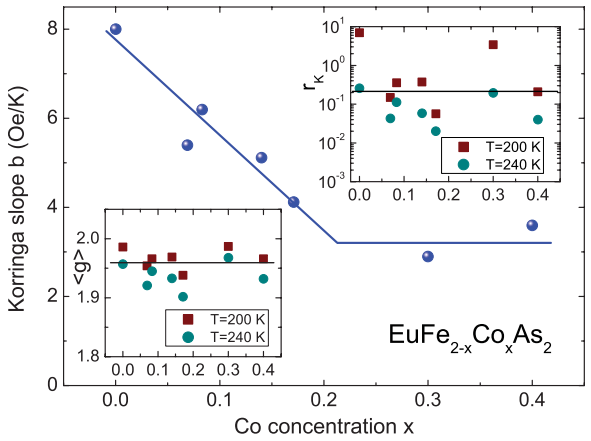

FIG. 6. (Color online) Concentration dependence of Korringa slope b (main frame) in the normal metallic regime, averaged g value $\langle g \rangle$ at 200 and 240 K (lower inset), and corresponding Korringa ratio r_K (upper inset) in $EuFe_{2-x}Co_xAs_2$. Solid lines are drawn to guide the eye.

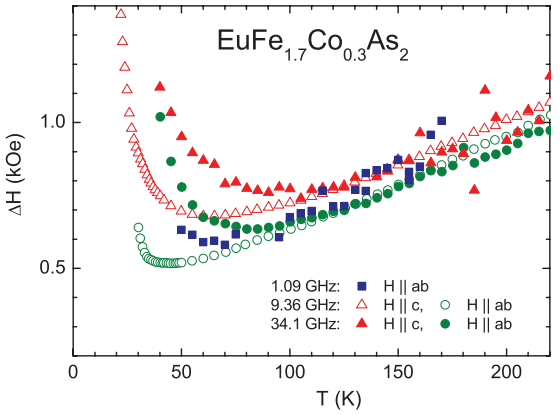

FIG. 7. (Color online) Temperature dependence of the linewidth in $EuFe_{1.7}Co_{0.3}As_2$ for the magnetic field aligned along the principal axes at three different microwave frequencies.

in such a way that $1/(T_1T)$ vs T exhibits a positive curvature.[61] The deviations from a linear temperature dependence in both ESR linewidth and nuclear spin-lattice relaxation rate are probably related to the unconventional linear increase of the conduction-electron susceptibility, as observed in iron pnictides such as $BaFe_{2-x}Co_xAs_2$ or LaFeAsO,[7] which is in contrast to the temperature-independent Pauli susceptibility of usual metals. These findings are further supported by the temperature dependence of the resonance field.

For all Co concentrations under investigation the resonance field slightly increases with increasing temperature above T_{SDW}. As already observed in pure $EuFe_2As_2$ the resulting g shift is negative with respect to the insulator value $g = 1.993$ and its absolute value increases with temperature. As in usual metals the g shift is a local probe for the Pauli susceptibility of the conduction electrons,[56]

$$\Delta g = J(0)N(E_F) \propto \chi_{Pauli}; \tag{2}$$

in the present case such a linear increase of the g value is again in accord with the linear increase of the conduction-electron susceptibility. At the same time the g shift matches the linear temperature increase of the ^{75}As Knight shift found in the NMR investigations of $BaFe_{2-x}Co_xAs_2$.[61]

However, it is important to mention that in the case of broad resonance lines one has to be careful with the absolute value of the resonance shift, because the D/A ratio and resonance field H_{res} are usually not fully independent parameters in such a way that an increase of D/A results in a concomitant decrease of H_{res}, i.e., an increase of g value. Especially for $T > 250$ K, the resonance shift is accompanied by a significant drop of the D/A ratio and the resulting g shift $|\Delta g| > 0.1$ appears to be too large regarding the Korringa ratio

$$r_K = \frac{g\mu_B}{\pi k_B}\frac{b}{(\Delta g)^2}, \tag{3}$$

which is expected to be ~ 1 in the case of s character and ~ 0.2 in the case of d character of the Fermi surface.[62] For $x = 0$ with $b \approx 8$ Oe/K and $\Delta g \approx -0.04$ (determined at 240 K sufficiently above the SDW transition) we find $r_K \approx 0.21$ suggesting that the Eu spin basically couples to the d electrons. As shown in the upper inset of Fig. 6, for all other Co concentrations the Korringa ratio determined from the g value averaged over the three principal axes at two temperatures (200 and 240 K, shown in the lower inset of the same figure) and the average of the Korringa slope b also scatters around $r_K = 0.2$ but with large uncertainties. Thus one should not overinterpret its meaning.

It is more important to return to the linewidth data. Recent ESR experiments by Garcia *et al.*[63] performed on polycrystalline $EuFe_{2-x}Co_xAs_2$ stated a significant frequency dependence of the Korringa slope in the regime $1 \leqslant \nu \leqslant 34$ GHz suggesting some kind of bottleneck scenario. In case of a so-called bottleneck the coupling between Eu spins and conduction electrons would be stronger than the coupling of the conduction electrons to the lattice, i.e., the microwave energy absorbed by the Eu spins is retained in the magnetic system of Eu spins and conduction electrons and cannot flow fast enough to the lattice. In such a case the Korringa slope depends on the experimental parameters such as microwave frequency or concentration of Eu spins which mask the pure effect of the electronic density of states.[56] We therefore investigated a single crystal with Co concentration $x = 0.3$, where the linear Korringa regime extends over the broadest temperature range compared to the other concentrations, at three frequencies 1.09 (L), 9.36 (X), and 34.1 GHz (Q band). As one can see in Fig. 7, above 100 K the linewidth data taken at different frequencies basically coincide with each other. For X and Q bands both for $H||c$ as well as $H \perp c$, we observe the same Korringa slope up to about 200 K. At higher temperature, the signal quality was not satisfying any more at Q-band frequency because of the smaller skin depth as compared to X band. Below 100 K the linewidth starts to increase with decreasing temperature. This effect is stronger at Q-band frequency than at X-band due to the larger polarization of the Eu spins in the higher resonance field. L-band data could only be obtained for the orientation of smallest linewidth $H \perp c$, because the sensitivity is much weaker than in the X band. Again the observed Korringa slope agrees with that of the higher frequencies within experimental uncertainties in contrast to the strong increase of the linewidth,

which was reported for polycrystalline material.[63] Thus, our data unequivocally discard a bottleneck scenario and strongly favor the pure Korringa-relaxation process. The reason is not clear at the moment, but maybe surface effects dominate in the powder samples reported in Ref. 63. Another proof for the Korringa process will be given when considering the strontium diluted crystals below.

B. P substitution on the As site

Before discussing the case of crystals with dilution at the Eu site, we shortly compare the case of P substitution on the As site. Figure 8 shows the evolution of the ESR spectra in $EuFe_2As_{2-y}P_y$ with increasing P concentration. Again the spectra are well described in terms of a single Dyson line. The temperature dependence of linewidth and resonance field is depicted in Fig. 9. For $y = 0.28$ the characteristics of the SDW still show up below $T_{SDW} \approx 80$ K. This means that in case of isoelectronic substitution (As by P) one needs about twice the concentration to suppress the SDW as compared to the electron doping case (Fe by Co). No SDW is formed for the sample with $y = 0.43$.

On increasing temperature an additional broad background signal becomes visible, which probably results from small amounts of residual ferromagnetic clusters ($< 1\%$) below the sensitivity of x-ray diffraction. This signal strongly disturbs the evaluation of the ESR spectra above 150 K, and therefore the results have to be considered with care at those temperatures. At least one can state that the slope of the linewidth in the usual metallic regime is reduced in a similar way as in the case of Co substitution.

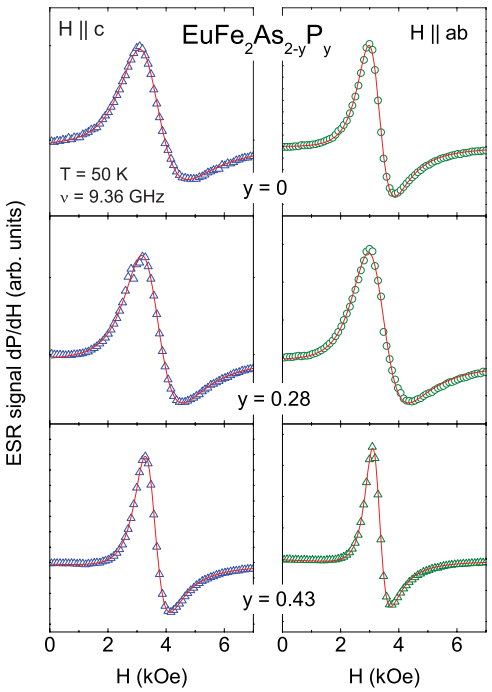

FIG. 8. (Color online) ESR spectra and corresponding fit curves for single crystals of $EuFe_2As_{2-y}P_y$ with $y = 0$ (upper), 0.28 (middle), and 0.43 (lower frames) at $T = 50$ K for the magnetic field applied parallel (left column) or perpendicular (right column) to the tetragonal c axis.

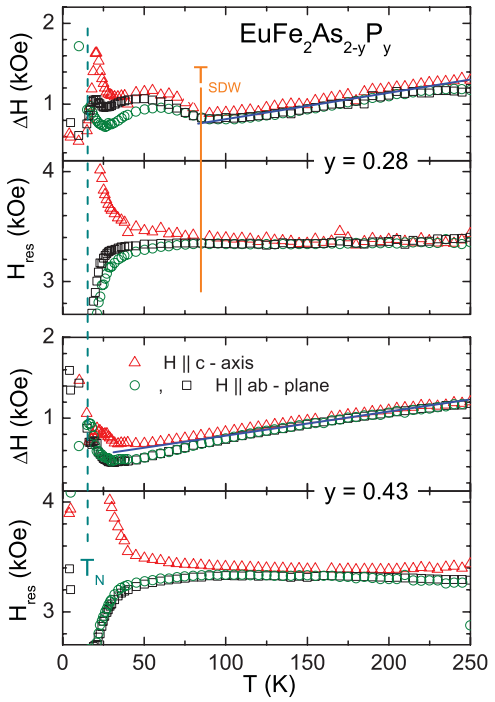

FIG. 9. (Color online) Temperature dependence of the ESR linewidth ΔH in $EuFe_2As_{2-y}P_y$ for $y = 0.28$ and $y = 0.43$. The SDW transition (T_{SDW}) and the magnetic ordering transition of the Eu spins (T_N) are marked by vertical lines. The blue solid lines indicate the linear Korringa law.

Moreover it is important to note that for both P concentrations under consideration the increase of the linewidth with increasing temperature turns out to be really linear as in a usual metal. At the same time the g shift from the insulator value is approximately temperature independent indicating a constant Pauli susceptibility. Indeed, this is fully in accordance with the ^{31}P NMR spin-lattice relaxation rate and Knight shift in $BaFe_2As_{2-y}P_y$. The former approaches a linear Korringa law in the normal metallic regime, while the latter resembles a temperature-independent Pauli susceptibility.[64] These results indicate that—in contrast to the Co substitution—P substitution drives the material rather into a normal Pauli-like metallic state. Indeed dissimilarities of the electronic structures between Co and P substitution were pointed out based on ARPES experiments in $EuFe_2As_{2-y}P_y$.[65]

Looking closer to the ESR spectra below $T < 30$ K for $y = 0.43$ reveals a splitting of the signal already significantly above the magnetic ordering temperature of the Eu spins. Here the signal can be satisfactorily described by two resonance lines as illustrated in Fig. 10. The ESR parameters of the first line (triangles) reveal clear anomalies at the superconducting transition $T_c = 25$ K.[13] The intensity flattens and decreases to lower temperatures, while the linewidth develops a peak with a maximum at 22 K. The second line (squares) appears at about 30 K and its intensity and linewidth both significantly increase down to the magnetic ordering temperature T_N of the Eu spins, where they exhibit a kink before slightly decreasing to lower temperatures. This observation suggests the coexistence of superconducting (line 1) and magnetically ordered (line 2) regimes. As recently reported by several

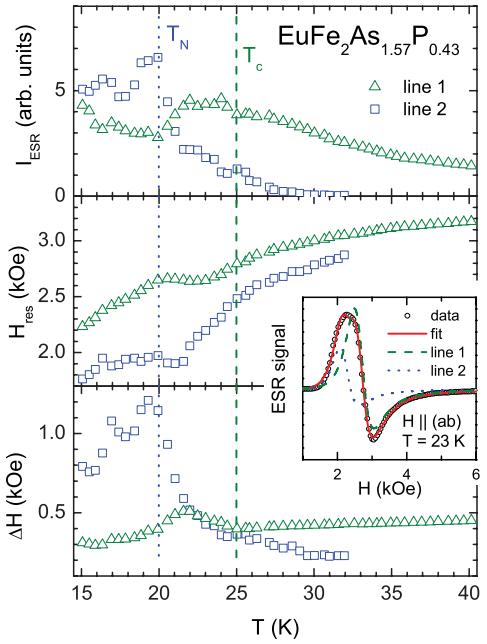

FIG. 10. (Color online) Temperature dependence of the ESR intensity, resonance field, and linewidth ΔH in $EuFe_2As_{1.57}P_{0.43}$ obtained from a fit by the sum of two resonance lines. Inset: ESR signal and fit curves at $T = 23$ K. Superconducting transition (T_c) and the magnetic ordering transition of the Eu spins (T_N) are marked by vertical lines.

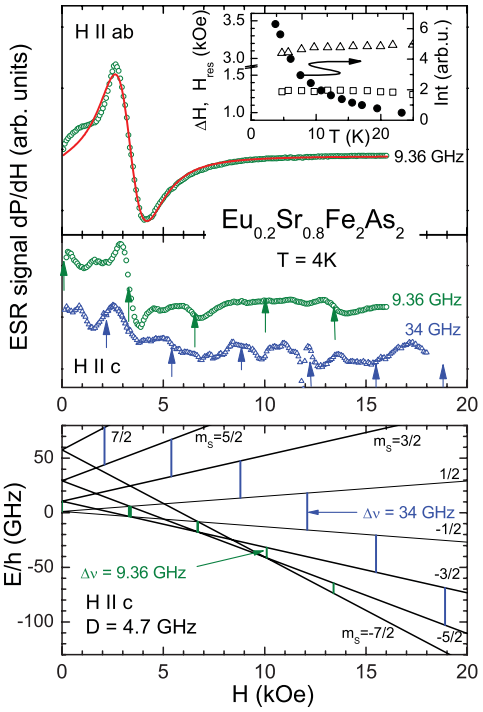

FIG. 11. (Color online) ESR spectra and corresponding fit curves for a single crystal of $Eu_{0.2}Sr_{0.8}Fe_2As_2$ at $T = 4$ K for the magnetic field applied perpendicular (upper frame, X band) and parallel (middle frame, X and Q bands) to the tetragonal c axis. The lower frame shows the Zeeman splitting of the ground state for the case of a zero-field splitting $D = 4.7$ GHz with the corresponding magnetic dipolar transtions at X-band and Q-band frequencies. Inset: temperature dependence of ESR intensity (solid spheres), resonance field (open triangles), and linewidth (open squares) for $H \perp c$.

authors, magnetization and resistivity,[33] magnetic Compton scattering,[34] and Mössbauer studies,[35] indicate the coexistence and competition of superconductivity and ferromagnetism, which sets in already on the right wing of the superconducting dome.[36] Moreover, the peak below T_c observed in the linewidth of the first line can be interpreted in terms of a Hebel-Slichter peak, expected in superconductors with an isotropic BCS-type gap. This corroborates the findings of recent optical investigations, which revealed BCS-type s-wave superconductivity without nodes in $EuFe_2As_{1.64}P_{0.36}$.[37] Thus, in the case of P substitution the superconducting phase is obviously of different character than in $Eu_{0.5}K_{0.5}Fe_2As_2$ and in Co-substituted (Eu,Sr)Fe_2As_2, which will be discussed in the following section.

C. Sr substitution on the Eu site

To reduce the influence of the europium spins we diluted the Eu^{2+} ions by substitution of about 80% isovalent Sr^{2+} ions both in the SDW mother compound and in a superconducting sample with 14% Co on the Fe site. To start with the SDW compound, Fig. 11 shows spectra at $T = 4$ K for the magnetic field applied parallel as well as perpendicular to the crystallographic c axis. While in the latter case the spectrum appears to be reasonably exchange narrowed (upper frame), a partially resolved fine structure shows up for the former field configuration. The lower frame shows a simulation of the magnetic dipolar transitions for $H||c$ due to the purely axial zero-field splitting term $H_{CF} = DS_z^2$ which modifies the Zeeman energy levels correspondingly as

$$E(H,m_S) = g\mu_B H m_S + D m_S^2, \qquad (4)$$

with $m_S = -7/2, -5/2, \ldots, 7/2$. For the calculation we used the axial parameter $D = 4.7$ GHz, which simultaneously approximates the observed splitting both for X- and Q-band frequency and is in agreement with $D = 5.5$ GHz obtained from the evaluation of the linewidth anisotropy in $EuFe_2As_2$.[48] As the all-over zero-field splitting $\Delta\nu_{ZFS} = 12D = 56.4$ GHz is much larger than the X-band frequency of $\nu = 9.36$ GHz, the transitions basically occur in the lower part of the diagram and partially overlap, while for the higher Q-band frequency the transitions appear already in the right order, but cannot be followed up to the highest resonance field because of the limit of the electromagnet. Deviations may occur due to disorder of the random substitution, due to weak nonzero orthorhombic contributions $E(S_y^2 - S_x^2)$ to the zero-field splitting as well as from a slight misalignment ($< 3^\circ$) of the crystal.

The inset in the upper frame documents the temperature dependence of the ESR parameters obtained from the fit with a single Dyson line for $H \perp c$, which can be reasonably evaluated only up to about 25 K. At higher temperatures an impurity signal due to small amounts of ferromagnetic impurities dominates the spectrum. Besides the Curie-Weiss law of the intensity and the resonance field close to $g = 2$, the nearly constant linewidth $\Delta H = 1.3$ kOe has to be mentioned. This is in good agreement with the linewidth observed in the SDW regime and also does not exhibit any linear Korringa

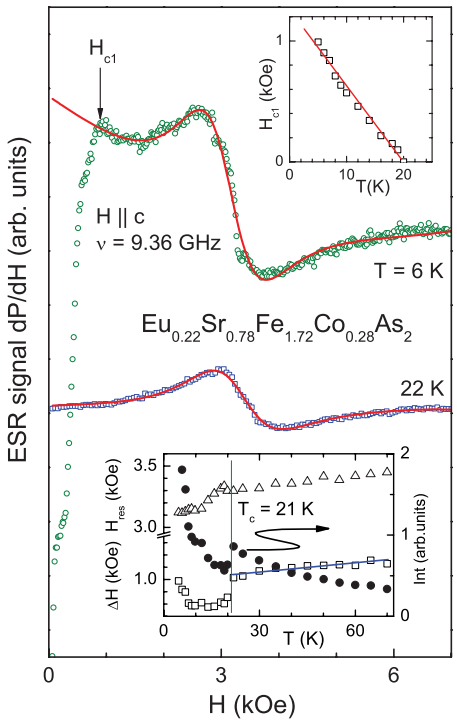

FIG. 12. (Color online) ESR spectra and corresponding fit curves of a single crystal of $Eu_{0.22}Sr_{0.78}Fe_{1.72}Co_{0.28}As_2$ at $T = 4$ K for the magnetic field applied parallel to the tetragonal c axis. Upper Inset: lower critical field H_{c1} as a function of temperature. Lower inset: temperature dependence of ESR intensity (solid spheres), resonance field (open triangles), and linewidth (open squares).

law, which again indicates the decoupling between localized Eu spins and conduction electrons in this phase.

Characteristic spectra of the superconducting compound are depicted in Fig. 12 above and below the superconducting transition at $T_c = 20$ K. One observes a single exchange narrowed line which is again well described in terms of a Dyson line. In the superconducting regime at low magnetic fields a strong nonresonant microwave absorption due to changes in the diamagnetic susceptibility shows up, which allows the determination of the lower critical field H_{c1} at the transition from the Meissner phase into the Shubnikov phase, where magnetic flux enters the sample.[66] The upper inset shows the temperature dependence of H_{c1} which increases approximately linearly on decreasing temperature from T_c. The lower inset illustrates the temperature dependence of the ESR parameters of the paramagnetic resonance line. In the superconducting phase the broad high-field wing of the nonresonant absorption at magnetic fields above H_{c1} was empirically approximated by the field derivative of a Lorentz shape centered at zero field with a linewidth of the order of 10 kOe, which satisfactorily approximates the changes of the diamagnetic susceptibility in the Shubnikov phase. As in $Eu_{0.5}K_{0.5}Fe_2As_2$,[50] one clearly recognizes a drop in the intensity on cooling through T_c due to the shielding effect in the superconducting phase and a shift of the resonance field to g values $g \geqslant 2$. At the same time the linewidth drops at T_c without any coherence peak, ruling out a simple isotropic BCS scenario in agreement with recent NMR results.[44] However, the exact behavior close to T_c cannot be resolved because of the strong temperature dependence of the nonresonant microwave absorption at the onset of superconductivity. Nevertheless, the linear increase of the linewidth above T_c with a slope of $b = 3.3$ Oe/K agrees with that observed in $EuFe_{1.7}Co_{0.3}As_2$, thus proving the Korringa relaxation in the normal metallic phase and ruling out any bottleneck effect between the Eu spins and the conduction electrons, which would depend on the concentration of the Eu spins. Again a slight linear increase shows up in the resonance field indicating its relation to the linear increase of the conduction-electron susceptibility.

D. Comparison to Gd-1111

It is worthwhile to compare our results in Eu-122 compounds to those reported by Alfonsov *et al.*[67,68] on Gd-1111 compounds (Gd,La)FeAs(O,F) where the Gd^{3+} spins ($4f^7$, $S = 7/2$) are used as ESR probes. In the normal metallic phase of Gd-1111 the Korringa slope is one order of magnitude smaller than in Eu-122. The slope is practically independent of the Gd concentration ruling out any bottleneck effect and indicating that the conduction-electron density of states is much smaller at the rare-earth site in 1111 compounds as compared to 122 systems. In contrast to cobalt or phosphorous substitution in Eu-122 the Korringa slope is slightly increasing in Gd-1111 with substitution of fluorine on the oxygen site,[68] suggesting an increasing density of states at the rare-earth site. The transition into the spin-density wave state can be best identified for samples with only 2% or 5% Gd on the rare-earth site, where the crystal field provokes a significant increase of the linewidth, and even a resolved fine structure can be observed at low temperatures, indicating the uniaxial zero-field splitting parameter D to be about one order of magnitude smaller than in Eu-122. At the same time the Korringa relaxation is not suppressed in the SDW phase but its slope is comparable to that in normal metallic phase, i.e., the electronic density of states does not open a gap at the rare-earth site in Gd-1111. Moreover, no significant anomaly of linewidth or resonance field is identified at the SC transition in the F-substituted sample, indicating again the absence of any gap at the rare-earth site for Gd-1111 in contrast to Eu-122. In concentrated GdFeAs(O,F) the inhomogeneous broadening due to anisotropic exchange with the canted iron moments dominates the ESR properties to low temperatures, especially in the case of high-field high-frequency ESR, where the Korringa relaxation becomes entirely masked even in the normal metallic phase.[67]

IV. SUMMARY

As a central result the absence of any bottleneck effect in the Eu spin relaxation via the conduction electrons evidences the weak coupling between europium and iron spins in $EuFe_2As_2$ and corresponding Sr-, Co-, and P-substituted compounds. This is a necessary prerequisite to ensure that the magnetism of the Eu spins does not significantly influence the general physical properties of the conduction-electron system, except suppressing superconductivity at low temperatures.

Considering first the paramagnetic, normal metallic regime $T \geqslant (T_{SDW}, T_c)$, both g shift with respect to the insulator

value and increase of the linewidth with temperature due to the Korringa relaxation simultaneously probe the local susceptibility of the itinerant iron spins, which in a usual magnetization measurement is masked by the strong Curie-Weiss susceptibility of the Eu spins as well as by additional van Vleck and diamagnetic contributions. Thus, in the compounds under consideration only ESR allows the extraction of the pure iron spin susceptibility. In $EuFe_{2-x}Co_xAs_2$ the iron spin susceptibility turns out to increase linearly with temperature, while phosphorous substitution in $EuFe_2As_{2-y}P_y$ results in a Pauli-like temperature-independent spin susceptibility. Both findings are in agreement with the properties of the related Ba-based compounds.[61,64] The comparison of temperature increase of the linewidth and g shift (Korringa ratio) indicates the dominant d-electron character of the Fermi surface.

In the spin-density wave phase $T < T_{SDW}$ the ESR linewidth is only determined by the crystal-electric field of the ligands and the dipolar fields of neighboring Eu spins like in insulators, but no Korringa relaxation is observed despite high conductivity. This means that the part of the Fermi surface which is probed by the Eu spins opens a gap at T_{SDW} supporting the existence of a dropletlike Fermi surface without continuities along k_z derived from ARPES data.[21]

While in the Eu-concentrated compounds the superconducting properties remain masked due to the onset of magnetic order of the Eu spins close to 20 K, dilution of the europium spins by strontium substitution gives further insight: No coherence peak is observed in the temperature dependence of the linewidth close to the superconducting transition in $Eu_{0.22}Sr_{0.78}Fe_{1.72}Co_{0.28}As_2$ ruling out an isotropic BCS scenario and indicating the anisotropic structure of the superconducting energy gap like in the case of $Eu_{0.5}K_{0.5}Fe_2As_2$.[50] Moreover, from the nonresonant microwave absorption in the SC phase a linear increase of the lower critical field H_{c1} was detected on decreasing temperature.

Finally, indications of phase coexistence were detected in $EuFe_2As_{1.57}P_{0.43}$, where the ESR signal splits into two lines which can be ascribed to superconducting and magnetically ordered regimes, respectively. In contrast to the Co- and K-substituted compounds, a peak in the temperature dependence of the linewidth below T_c indicates a BCS-type scenario with an isotropic energy gap for P-substituted $EuFe_2As_2$.

ACKNOWLEDGMENTS

We thank Anna Pimenov and Vladimir Tsurkan for experimental support. We are grateful to Jörg Sichelschmidt and Tobias Förster (Max-Planck-Institut für Chemische Physik fester Stoffe, Dresden) for the opportunity to use the L-band spectrometer. We acknowledge financial support by the Deutsche Forschungsgemeinschaft (DFG) via SPP 1458 by project DE1762/1-1. The work at POSTECH has been supported by Basic Science Research Program (2010-0005669) and Max Planck POSTECH/KOREA Research Initiative Program (2011-0031558) through the National Research Foundation of Korea (NRF).

[1] Y. Kamihara, T. Watanabe, M. Hirano, and H. Hosono, J. Am. Chem. Soc. **130**, 3296 (2008).
[2] X. H. Chen, T. Wu, G. Wu, R. H. Liu, H. Chen, and D. F. Fang, Nature (London) **453**, 761 (2008).
[3] Z. A. Ren, W. Lu, J. Yang, W. Yi, X. L. Shen, Z. C. Li, GV. C. Che, X. L. Dong, L. L. Sun, F. Zhou, and Z. X. Zhao, Chin. Phys. Lett. **25**, 2215 (2008).
[4] M. Rotter, M. Tegel, and D. Johrendt, Phys. Rev. Lett. **101**, 107006 (2008).
[5] C. Kant, J. Deisenhofer, A. Günther, F. Schrettle, A. Loidl, M. Rotter, and D. Johrendt, Phys. Rev. B **81**, 014529 (2010).
[6] F.-C. Hsu, J.-Y. Luo, K.-W. Yeh, T.-K. Chen, T.-W. Huang, P. M. Wu, Y.-C. Lee, Y.-L. Huang, Y.-Y. Chu, D.-C. Yan, and M.-K. Wu, Proc. Natl. Acad. Sci. USA **105**, 14263 (2008).
[7] D. C. Johnston, Adv. Phys. **59**, 803 (2010).
[8] G. R. Stewart, Rev. Mod. Phys. **83**, 1589 (2011).
[9] H. S. Jeevan, Z. Hossain, D. Kasinathan, H. Rosner, C. Geibel, and P. Gegenwart, Phys. Rev. B **78**, 092406 (2008).
[10] A. S. Sefat, R. Jin, M. A. McGuire, B. C. Sales, D. J. Singh, and D. Mandrus, Phys. Rev. Lett. **101**, 117004 (2008).
[11] A. Leithe-Jasper, W. Schnelle, C. Geibel, and H. Rosner, Phys. Rev. Lett. **101**, 207004 (2008).
[12] Z. Ren, Q. Tao, S. Jiang, C. Feng, C. Wang, J. Dai, G. Cao, and Z. Xu, Phys. Rev. Lett. **102**, 137002 (2009).
[13] H. S. Jeevan, D. Kasinathan, H. Rosner, and P. Gegenwart, Phys. Rev. B **83**, 054511 (2011).
[14] H. Raffius, M. Mörsen, B. D. Mosel, W. Müller-Warmuth, W. Jeitschko, L. Terbüchte, and T. Vomhof, J. Phys. Chem. Solids **54**, 135 (1993).
[15] H. S. Jeevan, Z. Hossain, D. Kasinathan, H. Rosner, C. Geibel, and P. Gegenwart, Phys. Rev. B **78**, 052502 (2008).
[16] D. Wu, N. Barisic, N. Drichko, S. Kaiser, A. Faridian, M. Dressel, S. Jiang, Z. Ren, L. J. Li, G. H. Cao, Z. A. Xu, H. S. Jeevan, and P. Gegenwart, Phys. Rev. B **79**, 155103 (2009).
[17] J. Herrero-Martin, V. Scagnoli, C. Mazzoli, Y. Su, R. Mittal, Y. Xiao, Th. Brueckel, N. Kumar, S. K. Dhar, A. Thamizhavel, and L. Paolasini, Phys. Rev. B **80**, 134411 (2009).
[18] Y. Xiao, Y. Su, M. Meven, R. Mittal, C. M. N. Kumar, T. Chatterji, S. Price, J. Persson, N. Kumar, S. K. Dhar, A. Thamizhavel, and Th. Brueckel, Phys. Rev. B **80**, 174424 (2009).
[19] J. Koo, J. Park, S. K. Cho, K. D. Kim, S.-Y. Park, Y. H. Jeong, Y. J. Park, T. Y. Koo, K.-P. Hong, C.-H. Lee, J.-Y. Kim, B.-K. Cho, K. B. Lee, and H.-J. Kim, J. Phys. Soc. Jpn. **79**, 114708 (2010).
[20] S. J. Moon, J. H. Shin, D. Parker, W. S. Choi, I. I. Mazin, Y. S. Lee, J. Y. Kim, N. H. Sung, B. K. Cho, S. H. Khim, J. S. Kim, K. H. Kim, and T. W. Noh, Phys. Rev. B **81**, 205114 (2010).
[21] S. de Jong, E. van Heumen, S. Thirupathaiah, R. Huisman, F. Massee, J. B. Goedkoop, R. Ovsyannikov, J. Fink, H. A. Dürr, A. Gloskovskii, H. S. Jeevan, P. Gegenwart, A. Erb, L. Patthey, M. Shi, R. Follath, A. Varykhalov, and M. S. Golden, Europhys. Lett. **89**, 27007 (2010).

[22]B. Zhou, Y. Zhang, L.-X. Yang, M. Xu, C. He, F. Chen, J.-F. Zhao, H.-W. Ou, J. Wei, B.-P. Xie, T. Wu, G. Wu, M. Arita, K. Shimada, H. Namatame, M. Taniguchi, X. H. Chen, and D. L. Feng, Phys. Rev. B **81**, 155124 (2010).
[23]S. Jiang, Y. Luo, Z. Ren, Z. Zhu, C. Wang, X. Xu, Q. Tao, G. Cao, and Z. Xu, New J. Phys. **11**, 025007 (2009).
[24]M. Tokunaga, I. Katakura, N. Katayama, and K. Ohgushi, J. Low Temp. Phys. **159**, 601 (2010).
[25]T. Terashima, N. Kurita, A. Kikkawa, H. S. Suzuki, T. Matsumoto, K. Murata, and S. Uji, J. Phys. Soc. Jpn. **79**, 103706 (2010).
[26]C. F. Miclea, M. Nicklas, H. S. Jeevan, D. Kasinathan, Z. Hossain, H. Rosner, P. Gegenwart, C. Geibel, and F. Steglich, Phys. Rev. B **79**, 212509 (2009).
[27]T. Terashima, M. Kimata, H. Satusukawa, A. Harada, K. Hazama, S. Uji, H. S. Suzuki, T. Matsumoto, and K. Murata, J. Phys. Soc. Jpn. **78**, 083701 (2009).
[28]W. Uhoya, G. Tsoi, Y. K. Vohra, M. A. McGuire, A. S. Sefat, B. C. Sales, D. Mandrus, and S. T. Weir, J. Phys.: Condens. Matter **22**, 292202 (2010).
[29]N. Kurita, M. Kimata, K. Kodama, A. Harada, M. Tomita, H. S. Suzuki, T. Matsumoto, K. Murata, S. Uji, and T. Terashima, Phys. Rev. B **83**, 100501(R) (2011).
[30]N. Kurita, M. Kimata, K. Kodama, A. Harada, M. Tomita, H. S. Suzuki, T. Matsumoto, K. Murata, S. Uji, and T. Terashima, Phys. Rev. B **83**, 214513 (2011).
[31]K. Matsubayashi, K. Munakata, M. Isobe, N. Katayama, K. Ohgushi, Y. Ueda, Y. Uwatoko, N. Kawamura, M. Mizumaki, N. Ishimatsu, M. Hedo, and I. Umehara, Phys. Rev. B **84**, 024502 (2011).
[32]W. Uhoya, G. Tsoi, Y. K. Vohra, M. A. McGuire, and A. S. Sefat, J. Phys.: Condens. Matter **23**, 365703 (2011).
[33]G. Cao, S. Xu, Z. Ren, S. Jiang, C. Feng, and Z. Xu, J. Phys.: Condens. Matter **23**, 464204 (2011).
[34]A. Ahmed, M. Itou, S. Xu, Z. Xu, G. Cao, Y. Sakurai, J. Penner-Hahn, and A. Deb, Phys. Rev. Lett. **105**, 207003 (2010).
[35]I. Nowik, I. Felner, Z. Ren, G. H. Cao, and Z. A. Xu, J. Phys.: Condens. Matter **23**, 065701 (2011).
[36]S. Zapf, D. Wu, L. Bogani, H. S. Jeevan, P. Gegenwart, and M. Dressel, Phys. Rev. B **84**, 140503(R) (2011).
[37]D. Wu, G. Chanda, H. S. Jeevan, P. Gegenwart, and M. Dressel, Phys. Rev. B **83**, 100503(R) (2011).
[38]L. Sun, J. Guo, G. Chen, X. Chen, X. Dong, W. Lu, C. Zhang, Z. Jiang, Y. Zou, S. Zhang, Y. Huang, Q. Wu, X. Dai, Y. Li, J. Liu, and Z. Zhao, Phys. Rev. B **82**, 134509 (2010).
[39]Q. J. Zheng, Y. He, T. Wu, G. Wu, H. Chen, J. J. Ying, R. H. Liu, X. F. Wang, Y. L. Xie, Y. J. Yan, Q. J. Li, and X. H. Chen, J. Phys.: Condens. Matter **22**, 235701 (2010).
[40]Z. Guguchia, S. Bosma, S. Weyeneth, A. Shengelaya, R. Puzniak, Z. Bukowski, J. Karpinski, and H. Keller, Phys. Rev. B **84**, 144506 (2011).
[41]Z. Guguchia, J. Roos, A. Shengelaya, S. Katrych, Z. Bukowski, S. Weyeneth, F. Muranyi, S. Strässle, A. Maisuradze, J. Karpinski, and H. Keller, Phys. Rev. B **83**, 144516 (2011).
[42]A. Blachowski, K. Ruebenbauer, J. Zukrowski, Z. Bukowski, K. Rogacki, P. J. W. Moll, and J. Karpinski, Phys. Rev. B **84**, 174503 (2011).
[43]I. Nowik, I. Felner, Z. Ren, G. H. Cao, and Z. A. Xu, New J. Phys. **13**, 023033 (2011).
[44]R. Sarkar, R. Nath, P. Khuntia, H. S. Jeevan, P. Gegenwart, and M. Baenitz, J. Phys.: Condens. Matter **24**, 045702 (2012).
[45]Z. Ren, X. Lin, Q. Tao, S. Jiang, Z. Zhu, C. Wang, G. Cao, and Z. Xu, Phys. Rev. B **79**, 094426 (2009).
[46]Y. Qi, Z. Gao, L. Wang, D. Wang, X. Zhang, and Y. Ma, New J. Phys. **10**, 123003 (2008).
[47]A. Mitsuda, T. Matoba, F. Ishikawa, Y. Yamada, and H. Wada, J. Phys. Soc. Jpn. **79**, 073704 (2010).
[48]E. Dengler, J. Deisenhofer, H.-A. Krug von Nidda, Seunghyun Khim, J. S. Kim, Kee Hoon Kim, F. Casper, C. Felser, and A. Loidl, Phys. Rev. B **81**, 024406 (2010).
[49]J. J. Ying, T. Wu, Q. J. Zheng, Y. He, G. Wu, Q. J. Li, Y. J. Yan, Y. L. Xie, R. H. Liu, X. F. Wang, and X. H. Chen, Phys. Rev. B **81**, 052503 (2010).
[50]N. Pascher, J. Deisenhofer, H.-A. Krug von Nidda, M. Hemmida, H.S. Jeevan, P. Gegenwart, and A. Loidl, Phys. Rev. B **82**, 054525 (2010).
[51]V. Jaccarino, J. Appl. Phys. **32**, S102 (1961).
[52]M. Coldea, H. Schaeffer, V. Weissenberger, and B. Elschner, Z. Phys. B **68**, 25 (1987).
[53]T. Moriya, J. Phys. Soc. Jpn. **18**, 516 (1963).
[54]M. Hardiman, J. Pellisson, S. E. Barnes, P. E. Bisson, and M. Peter, Phys. Rev. B **22**, 2175 (1980).
[55]H.-A. Krug von Nidda, A. Schütz, M. Heil, B. Elschner, and A. Loidl, Phys. Rev. B **57**, 14344 (1998).
[56]S. E. Barnes, Adv. Phys. **30**, 801 (1981).
[57]J. P. Joshi and S. V. Bhat, J. Magn. Reson. **168**, 284 (2004).
[58]C. Kittel, Phys. Rev. **73**, 155 (1948).
[59]M. A. Tanatar, A. Kreyssig, S. Nandi, N. Ni, S. L. Budko, P. C. Canfield, A. I. Goldman, and R. Prozorov, Phys. Rev. B **79**, 180508(R) (2009).
[60]J.-H. Chu, J. G. Analytis, K. De Greve, P. L. McMahon, Z. Islam, Y. Yamamoto, and I. R. Fisher, Science **329**, 824 (2010).
[61]F. L. Ning, K. Ahilan, T. Imai, A. S. Sefat, M. A. McGuire, B. C. Sales, D. Mandrus, P. Cheng, B. Shen, and H.-H. Wen, Phys. Rev. Lett. **104**, 037001 (2010).
[62]D. Seipler and B. Elschner, Phys. Lett. A **55**, 115 (1975).
[63]F. A. Garcia, A. Leithe-Jasper, W. Schnelle, M. Nicklas, H. Rosner, and J. Sichelschmidt, New J. Phys. **14**, 063005 (2012).
[64]Y. Nakai, T. Iye, S. Kitagawa, K. Ishida, H. Ikeda, S. Kasahara, H. Shishido, T. Shibauchi, Y. Matsuda, and T. Terashima, Phys. Rev. Lett. **105**, 107003 (2010).
[65]S. Thirupathaiah, E. D. L. Rienks, H. S. Jeevan, R. Ovsyannikov, E. Slooten, J. Kaas, E. van Heumen, S. de Jong, H. A. Dürr, K. Siemensmeyer, R. Follath, P. Gegenwart, M. S. Golden, and J. Fink, Phys. Rev. B **84**, 014531 (2011).
[66]C. Rettori, D. Davidov, I. Belaish, and I. Felner, Phys. Rev. B **36**, 4028 (1987).
[67]A. Alfonsov, F. Muranyi, V. Kataev, G. Lang, N. Leps, L. Wang, R. Klingeler, A. Kondrat, C. Hess, S. Wurmehl, A. Köhler, G. Behr, S. Hampel, M. Deutschmann, S. Katrych, N. D. Zhigadlo, Z. Bukowski, J. Karpinski, and B. Büchner, Phys. Rev. B **83**, 094526 (2011).
[68]A. Alfonsov, F. Muranyi, N. Leps, R. Klingeler, A. Kondrat, C. Hess, S. Wurmehl, A. Köfiler, G. Behr, V. Kataev, and B. Büchner, J. Exp. Theor. Phys. **114**, 662 (2012).